PHYSICAL REVIEW A **80**, 040901(R) (2009)

Electron emission spectra of thermal collisions of He metastable atoms with Au(111) and Pt(111) surfaces: Evidence for Penning ionization

S. Masuda,[1] K. Sasaki,[1] M. Sogo,[1] M. Aoki,[1] and Y. Morikawa[2]
[1]*Department of Basic Science, Graduate School of Arts and Sciences, The University of Tokyo, Komaba, Meguro, Tokyo 153-8902, Japan*
[2]*The Institute of Scientific and Industrial Research, Osaka University, 8-1 Mihogaoka, Ibaraki, Osaka 567-0047, Japan*
(Received 6 April 2009; published 14 October 2009)

Electron emission spectra obtained by thermal collisions of $He^*(2^1S$ and $2^3S)$ atoms with Au(111) and Pt(111) surfaces were measured to clarify the electronically excited atom-metal interactions. It has been recognized that the metastable atoms de-excite on ordinary noble- and transition-metal surfaces via resonance ionization (RI) followed by Auger neutralization (AN) without no indication of Penning ionization (PI). Our data show that this traditional criterion partially breaks down in the He^*-Au(111) collision system. The local electronic states near the surface were examined by first-principles calculations using density functional theory. It reveals that the itinerant *sp* states are significantly spilled out toward the vacuum compared to the localized *5d* states, and their asymptotic features play a crucial role in determining the branching ratio between PI and RI+AN.

DOI: 10.1103/PhysRevA.80.040901 PACS number(s): 79.20.Rf, 73.20.−r

When a rare-gas atom in the long-lived electronically excited (metastable) state such as $He^*(2^3S)$ collides with a solid surface, it de-excites to the ground state accompanied by electron emission. This phenomenon was first reported by Oliphant in 1929 [1], and its basic understanding was developed by Hagstrum in the 1950s [2]: resonance ionization (RI) followed by Auger neutralization (AN) on metal surfaces and Penning ionization (PI) on insulator surfaces. Later, numerous experimental studies have been performed for well-defined noble-metal (Cu, Ag, and Au) and transition-metal (Fe, Ni, Mo, Ru, Pd, W, and Pt) surfaces [3], and concluded that the Hagstrum's criterion is valid, i.e., the RI+AN process operates on such high work function metal surfaces without any indication of PI [4]. Here, we show that this traditional criterion partially breaks down in the $He^*(2^1S)$ and $He^*(2^3S)$-Au(111) collision system.

Two types of decay channels of $He^*(2^3S)$ are schematically shown in the right panel of Fig. 1. On the noble- or transition-metal surfaces in which the conduction bands lie opposite the 2*s* level of $He^*(2^3S)$, the 2*s* electron tunnels resonantly and then the resulting $He^+(1^2S)$ ion is neutralized by an Auger transition. These processes are denoted by RI and AN, respectively. Since the AN process produces two holes in the valence bands, the electron emission spectrum reveals a broad structure reflecting the self-convolution of the local density of states. A generalized theory of AN has been reported by Valdés *et al.* [5]. The transition rate Γ for RI is governed by wave function overlap between the 2*s* state (ϕ_{2s}) of He^* and the conduction band (ϕ_c) of the surface,

$$\Gamma_{\mathrm{RI}} \propto \sum_{empty} |\langle \phi_{2s}(r)|\phi_c(r)\rangle|^2. \tag{1}$$

On insulator surfaces without empty state opposite the He^* 2*s* level, the RI process is suppressed and the PI process occurs instead, where an electron in the valence band (ϕ_v) of the surface fills the He^* 1*s* hole and the 2*s* electron is emitted to the continuum state (ϕ_E) simultaneously. In this case, a single hole is produced in the valence band, as in the case of photoemission. The transition rate for PI is given by

$$\Gamma_{\mathrm{PI}} \propto \sum_{\text{occupied}} \left| \langle \phi_v(r_1)\phi_{2s}(r_2)|\frac{1}{r_{12}}|\phi_{1s}(r_1)\phi_E(r_2)\rangle \right|^2 \tag{2}$$

This equation suggests that the electron transfer from the surface to the incident He^* atom depends largely on the differential overlap between ϕ_{1s} and ϕ_v. Since the metastable atom with a thermal translational energy (<0.1 eV) cannot penetrate into the bulk, an orbital exposed outside the surface gives more effective overlap than an orbital localized on the surface, yielding a stronger band in the spectrum. In principle, the PI process can occur also on the ordinary metal surface as a competing process of RI. However, the branching ratio, $\Gamma_{\mathrm{PI}}/\Gamma_{\mathrm{RI}}$, is usually very small because the He^* 2*s* orbital (effective radius r_{eff}=2.5 Å) [6] is much extent in space compared to the He^* 1*s* orbital (r_{eff}=0.3 Å) [7] and gives a more efficient overlap with metal wave function at a given distance from the surface [4].

The purpose of the preset study is twofold. One is to establish the occurrence of PI in the $He^*(2^1S$ and $He^*(2^3S)$-Au(111) system using metastable atom electron spectroscopy (MAES) [3,8,9], which is based on the energy analysis of electrons emitted by thermal collisions of He^* with a solid surface. As a reference, the MAES spectra of Pt(111) were measured under the same beam conditions. The observed ratio $(\Gamma_{\mathrm{PI}}/\Gamma_{\mathrm{RI}})$ was on the order of 10^{-2}-10^{-3} for Au(111) and much smaller for Pt(111). Another is to compare the spectroscopic findings with first-principles calculations. For this purpose, the local electronic states near the metal surfaces were calculated using density functional theory, and the transition rates of the relevant processes were analyzed by the asymptotic behavior of metal wave functions (without numerical calculations of the matrix elements in Eqs. (1) and (2)). The Au(111) surface is well known to reconstruct to form a superlattice (so-called $23\times\sqrt{3}$ herringbone reconstruction) [10]. Also the valence electronic structures, including the Shockley surface states in the projected band gap, have been investigated by ultraviolet photoemission spectroscopy (UPS) [11–13], scanning tunneling mi-

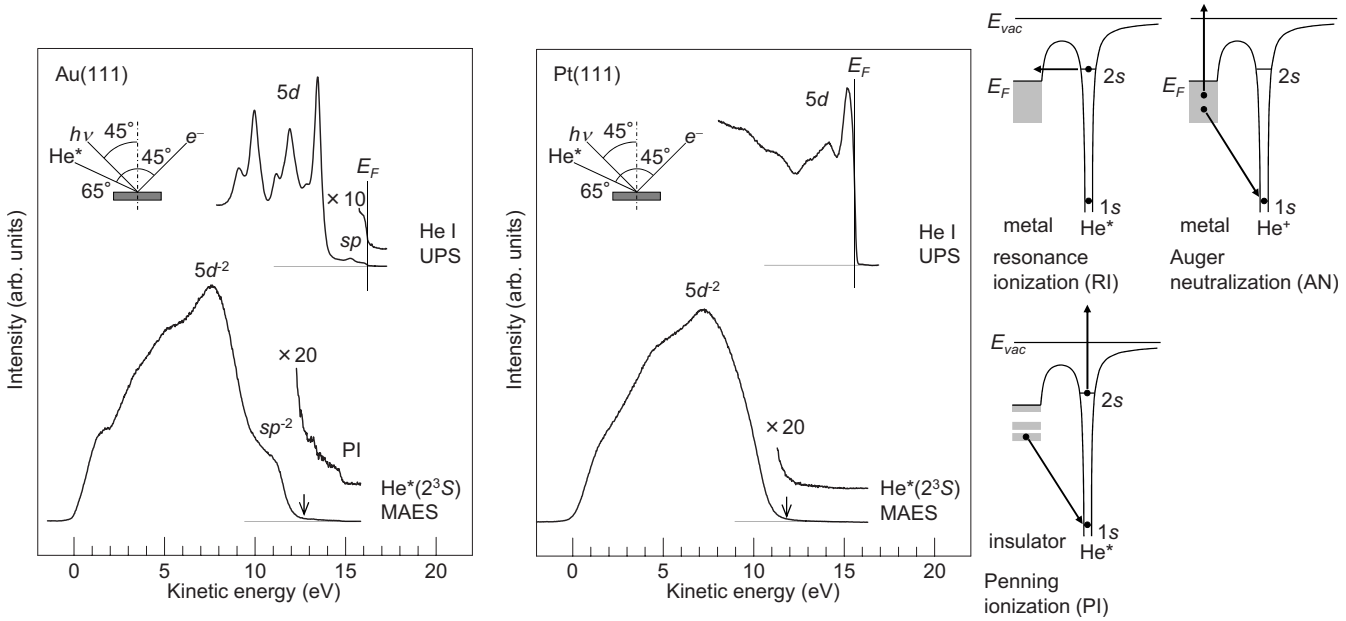

FIG. 1. He I UPS and He*(2^3S) MAES spectra of Au(111) and Pt(111) surfaces. The vertical arrow indicates the leading edge of electron emission via AN. The right panel shows two types of de-excitation channel of He*(2^3S) on a solid surface.

croscopy (STM) [14], and theoretical calculations [15,16]. The itinerant *sp* states are significantly spilled out toward the vacuum than the localized 5*d* states, which plays a crucial role in determining the branching ratio between PI and RI +AN.

The experimental setup and related procedure are reported elsewhere [17]. The Au(111) and Pt(111) surfaces were cleaned by repeated Ar^+ ion sputtering and heating cycles, and checked by Auger electron spectroscopy and low energy electron diffraction. The He*(2^1S, 20.62 eV) and He*(2^3S, 19.82 eV) atoms were produced by cold discharge and their intensity ratio was 6:94 at the sample position. The 2^1S atoms were quenched by a He discharge lamp (2.06 μm radiation) and the 2^3S spectrum was obtained. The 2^1S spectrum was derived by the difference between the two spectra taken with quench lamp on and off. The first-principles calculations based on a generalized gradient approximation in density functional theory were performed using a program package "STATE" (simulation tool for atom technology) [18]. We employed ultrasoft pseudopotential with plane wave basis set. The cutoff energies for wave functions and charge density are set to 25 and 225 Ry, respectively. A repeated slab model was applied, with each slab composed of 25 layers, separated by a vacuum region of 14.4 Å. In the present calculations, we assumed the 1×1 structure both for Au(111) and Pt(111). According to the first-principles calculations for reconstructed Au(111), the surface band structures are very similar for the top layer occupying fcc, hcp, and bridge sites [15].

Figure 1 shows the typical MAES spectra of Au(111) and Pt(111) using the He*(2^3S) atoms together with the He I UPS spectra. To facilitate comparison between the UPS and MAES spectra, the energy scale is given by the kinetic energy (E_k) of emitted electrons. The maximum E_k in the UPS spectra corresponds to the Fermi level (E_F). The UPS spectra of both surfaces have been measured several times and the assignments, including the two-dimensional surface states on Au(111) emerged in the projected band gap [11–13], are now well established. In our spectra, the intense 5*d* bands of Au(111) and Pt(111) appear at 2.5–7 and 0–6 eV below E_F, respectively, whereas the weak *sp* band of Au(111) appears just below E_F. The MAES spectrum of Pt(111) is essentially identical to the previous data by Hemmen and Conrad [19]. A broad structure with the leading edge at $E_k=11.8$ eV is due to the two-hole state of the 5*d* bands, $5d^{-2}$, produced via the RI+AN process. There is no indication of PI even in the magnified spectrum, as in the cases of the transition-metal (Fe, Ni, Mo, Ru, and W) and noble-metal (Cu, Ag, and Au) surfaces [3]. The RI+AN process takes place also on Au(111) as a dominant channel, yielding a broad structure with the leading edge at $E_k=12.7$ eV. Two bands centered at $E_k=10.5$ and 7 eV are mainly due to the two-hole states of the *sp* and 5*d* bands, respectively. However, as can be seen in Fig. 1, a weak band emerges at the higher E_k and is attributable to direct emission from the *sp* band via PI. A similar band via PI has been observed in the He*(2^3S) MAES spectrum of polycrystalline Au [20].

To confirm PI on Au(111) more directly, the He*(2^3S) and He*(2^1S+2^3S) spectra were measured with quench lamp on and off, respectively. The close-up spectra near E_F are shown in Fig. 2. The photoemission signals are due to small amounts of the He I resonance line containing in the metastable beams. The 2^1S and 2^3S spectra reveal the clear Fermi edge, whose positions in the E_k scale are shifted by 0.7 and 1.5 eV relative to that produced by the He I resonance line, respectively. These shifts are in good agreement with the difference in the excitation energies, i.e., $21.22(\text{He I})-20.62(2^1S)=0.60$ eV and $21.22(\text{He I})-19.82(2^3S)=1.40$ eV. Furthermore, the intensity ratio at the Fermi edge in the 2^1S and 2^3S spectra is about 1:10, which corresponds

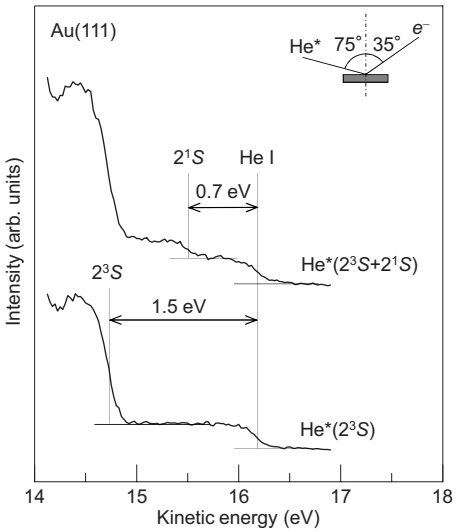

FIG. 2. $He^*(2^3S)$ and $He^*(2^1S$ and $2^3S)$ spectra of Au(111) surface measured with quench lamp on and off, respectively.

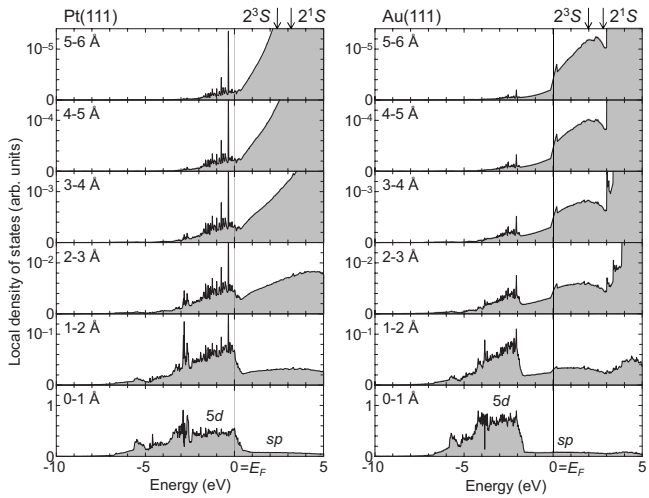

FIG. 3. Calculated local density of states for Pt(111) and Au(111) surfaces as a function of distance from the topmost metal layer (R). The integrated regions over R are shown in each panel. The vertical arrows stand for the lower limit of the $2s$ level of $He^*(2^3S)$ and $He^*(2^1S)$ approaching the metal surface (see text).

to their concentration in the mixed beam. Judging from the relative intensity of the sp^{-1} state via PI and the sp^{-2} states via RI+AN in Fig. 1, the branching ratio, Γ_{PI}/Γ_{RI}, is on the order of 10^{-2}-10^{-3}.

In order to analyze the above findings, we mention first the electronic states of He^* approaching a metal surface in a phenomenological way. The ionization energy of the $2s$ electron of He^* in front of the surface is approximated by $I_{eff}(He^*)=I_{eff}(He)-E_{eff}(He^*)$, where $I_{eff}(He)$ and $E_{eff}(He^*)$ are the effective ionization energy of the ground-state He and the effective excitation energy of He^* near the surface, respectively. When the AN process involves two electrons at E_F, the emitted electron has the maximum kinetic energy, $E_k(\max)=I_{eff}(He)-2\phi$, where ϕ is the work function. Using the observed values, i.e., $\phi=5.7$ eV and $E_k(\max)=11.8$ eV for Pt(111); $\phi=5.2$ eV and $E_k(\max)=12.7$ eV for Au(111), $I_{eff}(He)$ is obtained to be 23.1–23.2 eV for both surfaces. These values are 1.4–1.5 eV lower than the gas-phase one (24.6 eV), mainly due to the metal screening [2–4,8]. If the image potential is simply expressed by $E_{image}=-e^2/4(R-d)$, where R is the perpendicular distance between the He^+ ion and the topmost metal layer, and d is the location of the image plane from the topmost layer (usually, d is taken to be 0.6 Å) [21,22], the AN process is initiated at $R=3.0-3.2$ Å. On the other hand, $E_{eff}(He^*)$ does not change from the gas-phase value within ± 0.1 eV as described above. Thus, $I_{eff}(He^*)$ are obtained to be 2.5–2.6 and 3.3–3.4 eV for the 2^1S and 2^3S states, respectively. These values correspond to the lower limit of $I_{eff}(He^*)$ in which the RI process occurs at the initiation point of AN. When the RI process proceeds far from the metal surfaces prior to the AN process, $I_{eff}(He^*)$ would increase with increasing R.

Next, we address the local electronic structures in front of the metal surfaces. Figure 3 shows the calculated density of states for Pt(111) and Au(111) as a function of distance from the top layer (R). The lower limit of the $2s$ level of $He^*(2^1S)$ and $He^*(2^3S)$ mentioned above is indicated in the figure. In the top layer of Pt(111), a prominent structure located below and above E_F is composed mainly of the localized $5d$ bands, and a weak structure above E_F is composed of the dispersive sp bands. With increasing R, the local density of $5d$ states (in particular those with the higher binding energy, E_B) is strongly damped. This feature can be understood by the analogy with the free electron model, where the wave function tail extending outside the surface is proportional to $\exp(-E_B^{1/2}R)$. The empty sp states also show an exponential attenuation, but the damping rate is much smaller due to their spatial delocalization. As a consequence, in the region far

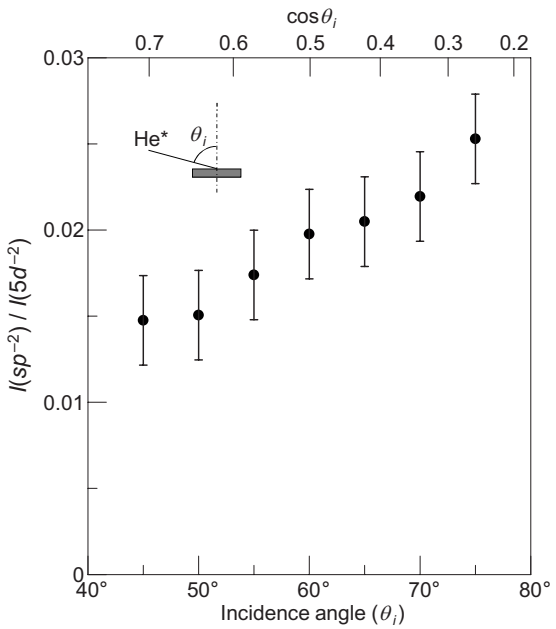

FIG. 4. Intensity ratio of the sp^{-2} and $5d^{-2}$ states, $I(sp^{-2})/I(5d^{-2})$, for Au(111) measured with different incidence angles (θ_i) of $He^*(2^3S)$. The access velocity of He^* (or He^+ in AN) to the surface is proportional to $\cos\theta_i$.

from the top layer ($R>3$ Å), the local density of empty *sp* states at 2–3 eV above E_F (corresponding to the 2*s* levels of He^*) is much higher than that of the filled 5*d* states, leading to the overwhelming operation of RI.

For Au(111), the 5*d* bands are located below E_F and the *sp* bands are extent crossing over E_F. The *sp* states are spilled further outside the top layer compared to the filled 5*d* states as in the case of Pt(111). However, the local density at 2–3 eV above E_F is apparently lower than that of Pt(111) mainly due to the presence of the projected band gap on Au(111). This causes the low tunneling probability of the He^* 2*s* electron to the empty *sp* states, eventually giving rise to the operation of PI. As is seen in Fig. 3, in the region far from the surface ($R>3$ Å), the local density of *sp* states attenuates by about one-tenth as *R* increases by 1 Å. Therefore, the local density of filled *sp* states in a certain point decreases from that of empty *sp* states of a point 2.2 Å away from the point by 100 times or more, where the separation corresponds to the difference between the effective radius of the 1*s* and 2*s* orbitals of $He^*(2^3S)$. This attenuation factor accords roughly with the observed branching ratio, Γ_{PI}/Γ_{RI}, although the numerical calculations of the matrix elements in Eqs. (1) and (2) are required for the detailed estimation.

Finally, we describe the local electronic states of Au(111) just outside the surface ($R<3$ Å), where the AN process takes place. Figure 4 shows the change in the intensity ratio of the sp^{-2} and $5d^{-2}$ states, $I(sp^{-2})/I(5d^{-2})$, measured with different incidence angles (θ_i) of $He^*(2^3S)$. The access velocity of He^* (or He^+ in AN) to the surface, $v_\perp$, is proportional to $\cos\theta_i$ and the dwell time across a certain distance, $\Delta R/v_\perp$, is inversely proportional to $\cos\theta_i$. It turns out from Fig. 4 that the intensity ratio increases monotonically with increasing incidence angle. In other words, when the access velocity becomes slow, the AN process is caused more efficiently by the outer-distributed *sp* electrons than the inner-distributed 5*d* electrons. This is in agreement with the asymptotic feature of the relevant local density of states shown in Fig. 3.

In conclusion, we demonstrate that the $He^*(2^1S$ and $2^3S)$ atoms de-excite on Au(111) partially via PI, in contrast to the cases of ordinary noble- and transition-metal surfaces. According to the first-principles calculations, the itinerant *sp* states are significantly exposed outside the surface compared to the localized 5*d* states, and their asymptotic features play a crucial role in the branching ratio between PI and RI + AN. The branching ratio depends also on the access velocity of He^* to the metal surface, as in the case of the formation of two-hole states in the AN process. Therefore, the PI process is not a specific event in collision of slow He^* atoms with Au(111), but would be a general one in collisions of fast He^* atoms with ordinary noble- and transition-metal surfaces.

We thank K. Makoshi for many interesting discussions. This study is financially supported through Special Coordination Funds of the Ministry of Education, Culture, Sports, and Science and Technology of the Japanese Government.

[1] M. L. E. Oliphant, Proc. R. Soc. London, Ser. A **124**, 228 (1929).
[2] H. D. Hagstrum, in *Electron and ion Spectroscopy of Solids*, edited by L. Fiermans, J. Vennik, and W. Dekeyser (Plenum, New York, 1978).
[3] Y. Harada, S. Masuda, and H. Ozaki, Chem. Rev. (Washington, D.C.) **97**, 1897 (1997), and references therein.
[4] W. Sesselmann, B. Woratschek, J. Küppers, G. Ertl, and H. Haberland, Phys. Rev. B **35**, 1547 (1987).
[5] D. Valdés, J. M. Blanco, V. A. Esaulov, and R. C. Monreal, Phys. Rev. Lett. **97**, 047601 (2006).
[6] P. E. Siska, Chem. Phys. Lett. **63**, 25 (1979).
[7] S. Fraga, J. Karwowski, and K. M. S. Saxena, *Handbook of Atomic Data* (Elsevier, Amsterdam, 1976).
[8] H. Morgner, Adv. At., Mol., Opt. Phys. **42**, 387 (2000).
[9] S. Krischok, P. Stracke, O. Höfft, V. Kempter, Yu. F. Zhukovskii, and E. A. Kotomin, Surf. Sci. **600**, 3815 (2006), and references therein.
[10] J. V. Barth, H. Brune, G. Ertl, and R. J. Behm, Phys. Rev. B **42**, 9307 (1990), and references therein.
[11] S. D. Kevan and R. H. Gaylord, Phys. Rev. B **36**, 5809 (1987).
[12] M. Hoesch, M. Muntwiler, V. N. Petrov, M. Hengsberger, L. Patthey, M. Shi, M. Falub, T. Greber, and J. Osterwalder, Phys. Rev. B **69**, 241401(R) (2004).
[13] S. LaShell, B. A. McDougall, and E. Jensen, Phys. Rev. B **74**, 033410 (2006).
[14] W. Chen, V. Madhavan, T. Jamneala, and M. F. Crommie, Phys. Rev. Lett. **80**, 1469 (1998), and references therein.
[15] N. Takeuchi, C. T. Chan, and K. M. Ho, Phys. Rev. B **43**, 13899 (1991).
[16] L. C. Davis, M. P. Everson, R. C. Jaklevic, and W. Shen, Phys. Rev. B **43**, 3821 (1991).
[17] M. Aoki, Y. Koide, and S. Masuda, J. Electron Spectrosc. Relat. Phenom. **156-158**, 383 (2007).
[18] Y. Morikawa, Phys. Rev. B **51**, 14802 (1995).
[19] R. Hemmen and H. Conrad, Phys. Rev. Lett. **67**, 1314 (1991).
[20] M. Aoki, S. Toyoshima, T. Kamada, M. Sogo, S. Masuda, T. Sakurai, and K. Akimoto, J. Appl. Phys. **106**, 043715 (2009).
[21] J. A. Appelbaum and D. R. Hamann, Phys. Rev. B **6**, 1122 (1972).
[22] J. Schmit and A. A. Lucas, Solid State Commun. **11**, 419 (1972).